

Diffusion of Asymmetric Swimmers

Andrew D. Rutenberg, Andrew J. Richardson, and Claire J. Montgomery

*Department of Physics and Atmospheric Science,
Dalhousie University, Halifax, Nova Scotia, Canada B3H 3J5*

(Dated: October 30, 2018)

Particles moving along curved trajectories will diffuse if the curvature fluctuates sufficiently in either magnitude or orientation. We consider particles moving at a constant speed with either a fixed or with a Gaussian distributed curvature magnitude. At small speeds the diffusivity is independent of the speed. At larger particle speeds, the diffusivity depends on the speed through a novel exponent. We apply our results to intracellular transport of vesicles. In sharp contrast to thermal diffusion, the effective diffusivity *increases* with vesicle size and so may provide an effective means of intracellular transport.

PACS numbers: 05.40.-a, 05.40.Fb, 87.16-b

The thermal Stokes-Einstein diffusivity of a sphere decreases as the particle radius R increases [1]. For this reason, while diffusive transport is used for individual molecules within living cells [2], larger objects such as vesicles and pathogens often use active means of transport. While many intracellular vesicles appear to be transported by molecular motors directed along existing cytoskeletal tracks [2, 5], *undirected* actin-polymerization mediated vesicle transport has been reported in some endosomes, lysosomes, other endogenous vesicles, and phagosomes [3, 4]. Active transport is also observed in the actin-polymerization-ratchet motility of certain bacteria [4, 14] and virus particles [6] within host cells. It is important to characterize the transport properties of vesicles that are not moving along pre-existing cytoskeletal tracks.

Existing discussions of the motion of actively propelled microscopic particles, or “swimmers”, assumes that in the absence of thermal fluctuations particles would move in straight trajectories [1, 7]. Thermal rotational diffusion will then randomly re-orient the trajectory [1], so that over long times diffusive transport will be observed. However in actin-polymerization based motility, particles appear to be attached to their long actin tails [8] which in turn are embedded in the cytoskeleton [9]. While thermal fluctuations will thereby be severely reduced, the actin-polymerization itself is a stochastic process with its own fluctuations [2, 10]. These intrinsic fluctuations can explain the observed curved trajectories, as well as the variation of the curvature over time [13]. The diffusivity of such asymmetrically moving particles has not been previously explored.

In this letter, we study asymmetric swimmers that would move in perfect circles in the absence of fluctuations. We examine both a “broken swimmer” with a fixed curvature magnitude and an axis of curvature that is re-oriented by fluctuations (rotating curvature, RC), and a “microscopic swimmer” with a normally-distributed curvature that is spontaneously generated by fluctuations (Gaussian curvature, GC). In both of these systems, fluctuations

lead to diffusion at long times. We use computer simulations to measure the diffusivity of these systems as a function of the root-mean-squared curvature K_0 , the particle speed v , and the timescale characterizing the curvature dynamics τ .

We obtain some exact results from polymer systems, where each polymer configuration represents a possible particle trajectory. Indeed, a broken swimmer with a fixed curvature magnitude in $d = 3$ is exactly analogous to the hindered jointed chain discussed by Flory [11] and we thereby recover the entire scaling function exactly. In that case, the diffusivity is independent of particle speed v . For Gaussian curvatures and for systems in restricted geometries ($d = 2$), the polymer analogy gives us the diffusivity only in the limit of slow speeds. At larger speeds, our simulations over 5 decades of speed show that diffusivity depends on particle speed with a non-trivial exponent λ . The diffusivity appears to be dominated by the occasional long straight segments of trajectory that occur when the curvature is small. Scaling arguments based on this observation are consistent with the measured exponent $\lambda_{2d} = 0.98 \pm 0.02$ in $d = 2$, but do not recover our measured exponent $\lambda_{3d} = 0.71 \pm 0.01$ in $d = 3$.

A curved path has a curvature magnitude $K \equiv 1/R$, where R is the instantaneous radius of curvature. If we describe a particle trajectory by a position $\mathbf{r}(t)$, then the vector curvature is defined by the cross-product $\mathbf{K} \equiv \mathbf{v} \times \dot{\mathbf{v}}/v^3$, where $v = |\mathbf{v}|$ is the speed and the dot indicates a time-derivative. For uniform motion around a circle, R is the radius of the circle, and \mathbf{K} is oriented perpendicular to the circle along the axis. We consider particles moving at a constant speed and with an instantaneous curvature \mathbf{K} , so that $\dot{\mathbf{r}} = \mathbf{v}$ and $\dot{\mathbf{v}} = -v\mathbf{v} \times \mathbf{K}$. For “rotating curvature” dynamics (RC) we fix the curvature magnitude $|\mathbf{K}| = K_0$ but allow the curvature to randomly rotate around the direction of motion:

$$\dot{\mathbf{K}}_{RC} = \xi \hat{\mathbf{v}} \times \mathbf{K} \quad (1)$$

where the unit-vector $\hat{\mathbf{v}} = \mathbf{v}/v$, the Gaussian noise ξ has zero mean, and $\langle \xi(t)\xi(t') \rangle = 2\delta(t - t')/\tau$ with a char-

acteristic timescale τ . This represents the simplest description of a mesoscopic swimmer that has a “locked-in” curvature due to, e.g., an asymmetric shape. For “Gaussian curvature” dynamics (GC) the curvature magnitude changes as well:

$$\dot{\mathbf{K}}_{GC} = -\mathbf{K}/\tau + \boldsymbol{\xi} \quad (2)$$

where the noise $\boldsymbol{\xi}$ is perpendicular to \mathbf{v} with zero mean and $\langle \boldsymbol{\xi}(t) \cdot \boldsymbol{\xi}(t') \rangle = \delta(t-t')K_0^2/\tau$, such that $\langle \mathbf{K}^2 \rangle = K_0^2$. This represents the simplest description of a microscopic swimmer “trying” to swim in a straight line subject to intrinsic fluctuations in the motion. The resulting curvatures are Gaussian distributed in each component. For particles restricted to two-dimensions with either RC or GC dynamics, we only use the normal (\hat{z}) component of the vector-curvature to update the velocity within the plane, i.e. $\dot{\mathbf{v}} = -v\mathbf{v} \times \hat{z}K_z$ in $d = 2$.

There are two natural timescales. We explicitly introduce τ , which controls the noise correlation and so sets the timescale over which the curvature changes. There is also the inverse of the angular rotation rate, $t_c \equiv 1/(vK_0)$. Diffusion will only be observed for elapsed times t much greater than any other timescale in the system, i.e. $t \gg t_c$ and $t \gg \tau$. The diffusivity of a particle is given by $D \equiv \langle r^2 \rangle / (2dt)$ in the limit as the elapsed time $t \rightarrow \infty$, in spatial dimension d .

A polymer chain with fixed bond lengths (ℓ) and angles (θ_f), and with independent bond rotation potentials ($V(\phi_f)$) [11] is statistically identical to the continuous RC trajectory in $3d$ if for a discrete time-step Δt we take $\ell = v\Delta t$. The end-to-end distance for a long n -bond polymer is $\langle r^2 \rangle = n\ell^2 C_n$. The correspondence is complete as the elapsed time $t = n\Delta t \rightarrow \infty$. The bond and dihedral angles determine $C_\infty = (1 + \cos\theta_f)(1 + \langle \cos\phi_f \rangle) / [(1 - \cos\theta_f)(1 - \langle \cos\phi_f \rangle)]$ [11]. Swimmers follow continuous paths, so we take the limit of small Δt and fix the polymer rotation angle from the curvature in that limit by $\theta_f = K_0 v \Delta t$, and rotate the curvature by $\langle \phi_f^2 \rangle = 2\Delta t/\tau$ in agreement with Eqn. 1. In the limit $\Delta t \rightarrow 0$ we recover the *exact* result $D = 1/(3K_0^2\tau)$ in $d = 3$. Remarkably, D is independent of v .

For a GC trajectory in $d = 3$, there is no obvious polymer analogy since the curvature magnitude evolves with time. In the limit of $\tau \rightarrow 0$ however, the curvature is independently Gaussian distributed at every point along the trajectory and the diffusivity can be extracted from the “worm-like chain” polymer model originally solved by Kratky and Porod [12]. The result is $D = 1/(3K_0^2\tau)$ in the limit of small τ . Note that the diffusivity diverges as $1/\tau$ so this is the leading asymptotic dependence for small τ . We obtain the same diffusivity for both RC and GC dynamics for small τ .

We use these exact results to define natural dimensionless scaling functions for the diffusivity of microscopic

swimmers:

$$\tilde{D}_{Rd,Gd}(\tilde{v}) \equiv DK_0^2\tau \quad (3)$$

where the index *Rd* or *Gd* indicates both the dynamics (RC or GC) and the spatial dimensionality d , and

$$\tilde{v} \equiv vK_0\tau \quad (4)$$

is a dimensionless speed. In terms of these scaling functions we have $\tilde{D}_{R3}(\tilde{v}) = \tilde{D}_{G3}(0) = 1/3$. The same Kratky-Porod approach in $d = 2$ gives $\tilde{D}_{R2}(0) = \tilde{D}_{G2}(0) = 1$.

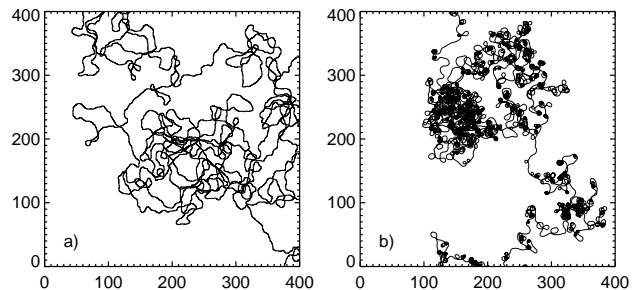


FIG. 1: a) Particle trajectory with GC dynamics in $d = 2$ with $\tilde{v} = 0.1$. The particle does not complete a circular loop before \mathbf{K} changes significantly. b) With $\tilde{v} = 100$. The particle can complete many circular loops before \mathbf{K} changes, however straight segments are seen when $|\mathbf{K}|$ is small. The result is a characteristic “knotty wool” appearance. In both cases $K_0 = 1$.

We have simulated the trajectories of large-numbers of independent particles with RC and with GC dynamics. For fixed v and K_0 , we varied τ to explore the scaled velocity $\tilde{v} \equiv vK_0\tau$ over 5 orders of magnitude. For each \tilde{v} , we averaged over the trajectories of at least 1000 particles. We explicitly integrated the dynamical equations using a simple Euler update with a small timestep Δt . In all cases $t \gg \tau \gg \Delta t$ and $t \gg t_c \gg \Delta t$, with separation of timescales by factors of 10 – 100. Systematic errors due to Δt and t are below our noise levels, and statistical errors (when not shown) are smaller than the size of our plotted points. Consistently, our numerical results agree with all exact results from the polymer analogy. We illustrate the trajectories that we observe in $d = 2$ in Fig. 1, with both small and large scaled speeds \tilde{v} . In both cases the curvature $K_0 = 1$, but particles only complete loops at large \tilde{v} . Qualitatively similar trajectories are seen in $d = 3$ with GC curvature dynamics.

In $d = 2$, shown in Fig. 2, both rotating curvature (open circles) and Gaussian curvature (filled circles) approach their asymptotic value of $\tilde{D}_{R2}(0) = \tilde{D}_{G2}(0) = 1$ at small \tilde{v} . At $\tilde{v} \approx 1$ there is a sharp cross-over to a large- \tilde{v} power-law regime, characterized by an exponent λ_{2d} where $\tilde{D}_{R2} \sim \tilde{D}_{G2} \sim \tilde{v}^{\lambda_{2d}}$ for large \tilde{v} . We show the effective exponents $\lambda_{eff} \equiv \Delta \log(DK_0^2\tau) / \Delta \log \tilde{v}$ between consecutive points in the inset of Fig. 2, as well as the

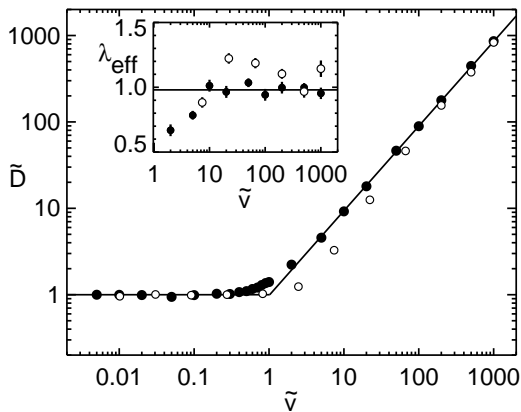


FIG. 2: Dimensionless diffusivities $\tilde{D} \equiv DK_0^2\tau$ for rotating (open circles, \tilde{D}_{R2}) and Gaussian (filled circles, \tilde{D}_{G2}) curvature dynamics in $d = 2$, plotted against dimensionless particle speed $\tilde{v} \equiv vK_0\tau$. Also shown with solid lines are the small \tilde{v} asymptote $\tilde{D} = 1$ and the large \tilde{v} best-fit asymptote $\tilde{D} \sim \tilde{v}^{\lambda_{2d}}$. The inset shows the effective exponents, with the solid line indicating the best-fit $\lambda_{2d} = 0.98 \pm 0.02$.

best fit exponent $\lambda_{2d} = 0.98 \pm 0.02$. We fit λ_{2d} from the large- \tilde{v} GC data only, due to the systematic cross-over remaining in the RC data even at large \tilde{v} .

Simulations in $d = 3$ with rotating curvature (RC) dynamics leads to a diffusivity in excellent agreement with the exact result from polymer physics, $\tilde{D}_{R3} = 1/3$, as shown by open circles in Fig. 3. Gaussian curvature dynamics (\tilde{D}_{G3} , filled circles) has the same behavior for small \tilde{v} , but exhibits a sharp crossover at $\tilde{v} \approx 1$ to a power-law regime $\tilde{D}_{G3} \sim \tilde{v}^{\lambda_{3d}}$ for large \tilde{v} . We find the best-fit exponent is $\lambda_{3d} = 0.71 \pm 0.01$, as shown by the solid line in the inset of Fig. 3. Because $\lambda_{3d} < 1$, this scaling curve may be used to uniquely identify the dynamical timescale τ if D , K_0 , and v are measured experimentally.

Is there a simple way of understanding the asymptotic behavior of \tilde{D} ? For RC dynamics in $d = 3$ the instantaneous curvature does not change in magnitude even while the curvature axis wanders. The particle will go in a circular trajectory, not contributing to diffusivity, until the curvature axis wanders significantly. The result is a random walk with step size given by the radius of curvature $\Delta r \sim 1/K_0$ and an interval between steps of τ , leading to $D \sim 1/(K_0^2\tau)$. This qualitatively explains why the exact result $\tilde{D}_{R3} = 1/3$ is independent of \tilde{v} .

It is more difficult to understand the $\tilde{D} \sim \tilde{v}^\lambda$ behavior for large \tilde{v} in the other systems. We start with a simple scaling argument based on the assumption that the relatively straight segments shown in Fig. 1 b) dominate the diffusivity. The interval between periods of small curvature should be on order the autocorrelation time τ . The length Δr of the straight segments are determined by how long the interval of small curvature lasts, Δt , since

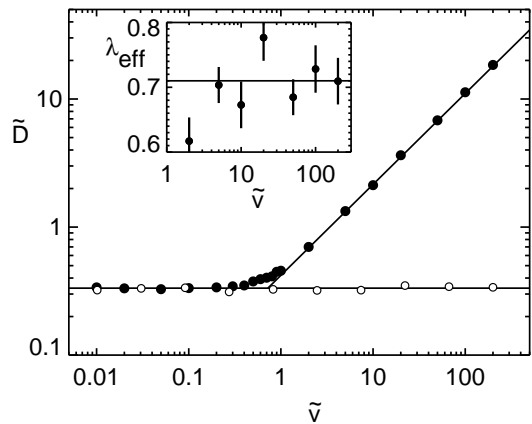


FIG. 3: Dimensionless diffusivities $\tilde{D} \equiv DK_0^2\tau$ for rotating (open circles, \tilde{D}_{R3}) and Gaussian (filled circles, \tilde{D}_{G3}) curvature dynamics in $d = 3$, plotted against dimensionless particle speed $\tilde{v} \equiv vK_0\tau$. Solid lines show the exact result $\tilde{D}_{R3} = 1/3$, as well as the large \tilde{v} power-law asymptote $\tilde{D}_{G3} \sim \tilde{v}^{\lambda_{3d}}$. The inset shows effective exponents between sequential points, with a solid line indicating the best-fit $\lambda_{3d} = 0.71 \pm 0.01$.

$\Delta r \approx v\Delta t$. For the segment to be straight, the curvature must be less than the inverse length, i.e. $K_{max} \lesssim 1/\Delta r$. The fraction of the time we have small curvature below K_{max} in magnitude should be proportional to the probability of having curvature below K_{max} . In $d = 2$ only the normal component of curvature affects the dynamics, so that $P(K) \approx \text{const}$ for $K \ll K_0$. This applies both to GC and RC. We therefore expect $\Delta t \sim \tau K_{max}/K_0$. We maximize K_{max} to maximize the contribution to $D \approx \Delta r^2/\tau$ and find $\tilde{D}_{G2} \sim \tilde{D}_{R2} \sim \tilde{v}$ as $\tilde{v} \rightarrow \infty$. This indicates that $\lambda_{2d} = 1$, which is consistent with our best-fit value $\lambda_{2d} = 0.98 \pm 0.02$. However, in $d = 3$ for GC dynamics the same argument leads to $\lambda_{3d} = 2/3$ since two Gaussian distributed components of the curvature gives $P_<(K_{max}) = \int_0^{K_{max}} dK P(K) \sim K_{max}^2/K_0^2$ for $K_{max} \ll K_0$. This is inconsistent with our measured value of $\lambda_{3d} = 0.71 \pm 0.01$, with a significant 4σ variation.

At what radius R_c does a small spherical particle achieve a higher diffusivity by actively swimming, as compared to passive thermal diffusion characterized by $D_T = k_B T / (6\pi\eta R)$ [1]? We can answer this question within the context of actin-polymerization based motility of small intracellular particles, since the size dependence of K_0 , v , and τ is known, at least approximately. With the approximation that n propulsive actin filaments are randomly distributed over a particle of size R , the curvature of the trajectory will be $K_0 \propto 1/(R\sqrt{n})$ [13]. With a size-independent surface-density of filaments we obtain $K_0 \approx A/R^2$, with a constant of proportionality A . By observations of *Listeria monocytogenes* we estimate $A \approx 0.1\mu\text{m}$ [13]. We also conservatively assume size-independent values for cytoplasmic viscosity $\eta \approx 3\text{Pa}\cdot\text{s}$ [1, 13], speed $v \approx 0.1\mu\text{m}/\text{s}$, and autocorrelation decay

time $\tau \approx 100s$ [15]. We find that the micron-scale bacterium *L. monocytogenes* has $\tilde{v} \approx 1$, so that smaller particles will have $\tilde{v} > 1$. Using the large \tilde{v} asymptotic behavior of \tilde{D}_{G3} shown in Fig. 3, $D \approx 0.41\tilde{v}^{\lambda_{3d}}/(K_0^2\tau)$, and the size-dependence $K_0 \approx A/R^2$, we obtain

$$D_{G3} \sim R^{4-2\lambda_{3d}}v^{\lambda_{3d}}/(A^{2-\lambda_{3d}}\tau^{1-\lambda_{3d}}), \quad (5)$$

with a measured $\lambda_{3d} = 0.71 \pm 0.01$. In dramatic contrast to thermal diffusion, D increases with increasing particle size. Comparing with D_T we find that for all sizes above $R_c \approx 80nm$ a particle will have a higher diffusivity by actively swimming by the actin-polymerization mechanism than by passive thermal diffusion. Provocatively, this is in the middle of the vesicle-size distribution seen in neural systems [16].

Our treatment of microscopic swimmers has ignored thermal fluctuations. A “rocket” traveling straight at speed v that is re-oriented only by thermal effects will have $D_u = 4\pi\eta R^3v^2/(3k_B T)$ [1]. In comparison with our results for D , we find that $D < D_u$ for particles larger than $R_u \approx 0.07nm$. For actin-polymerization based motility, intrinsic fluctuations appear to dominate thermal fluctuations at the particle sizes where active transport is advantageous.

In summary, we find that diffusivities of asymmetric microscopic swimmers depends on whether the swimmers are restricted to $2d$ or $3d$, and whether they have fixed asymmetries (RC) or the asymmetries are spontaneously generated (GC). Diffusivities are independent of particle speed at low speeds, in agreement with analogous polymer systems. At higher speeds an anomalously large diffusivity is observed that depends on the particle speed by \tilde{v}^λ where $\lambda_{2d} = 0.98 \pm 0.02$, in agreement with a scaling argument for $\lambda_{2d} = 1$. However $\lambda_{3d} = 0.71 \pm 0.01$, which significantly differs from our simple scaling result in $d = 3$. We apply our results to intracellular bacteria, virus particles, and vesicles that move via actin-polymerization. We find that diffusivities due to asymmetric swimming exceed thermal diffusivities for particles larger than approximately $80nm$. As a result asymmetric swimming may provide a viable intracellular transport mechanism even for vesicle-sized particles. We find

that for the relevant dynamics (GC in $d = 3$), diffusivities should increase with particle size, speed, and filament turnover rate, and also with smaller curvatures for a given size. It is interesting that the bacterium *Rickettsiae rickettsii* exhibits actin-polymerization intracellular motility with smaller intra-cellular speeds but straighter trajectories [13, 14] — raising the question of whether maximal diffusivity is selected for in this or other biological systems.

This work was supported financially by an NSERC discovery grant. C. Montgomery would also like to acknowledge support from an NSERC USRA.

-
- [1] H.C. Berg, “Random Walks in Biology”, 2nd ed. (Princeton, 1993).
 - [2] B. Alberts *et al.*, “Molecular Biology of the Cell”, 4th ed. (Garland, 2002).
 - [3] J. Taunton *et al.*, J. Cell. Biol. **148**, 519 (2000); C.J. Merrifield *et al.*, Nature Cell. Biol. **1**, 72 (1999); A.L. Rozelle *et al.*, Curr. Biol. **10**, 311 (2000); F.L. Zhang *et al.*, Cell. Motil. Cyto. **53**, 81 (2002).
 - [4] For reviews see L.A. Cameron *et al.*, Nature Rev. Mol. Cell Biol. **1**, 110 (2000); D. Pantaloni *et al.*, Science **292**, 1502 (2001); F. Frishnecht and M. Way, Trends Cell Biol. **11**, 30 (2001).
 - [5] N. Hirokawa, Science **279**, 519 (1998).
 - [6] S. Cudmore *et al.*, Nature **378**, 636 (1995).
 - [7] P.S. Lovely and F.W. Dahlquist, J. Theor. Biol. **50**, 477 (1975).
 - [8] F. Gerbal *et al.*, Eur. Biophys. J. **29**, 134 (2000).
 - [9] J.A. Theriot *et al.*, Nature **357**, 257 (1992).
 - [10] A. Mogilner and G. Oster, Biophys. J. **71**, 3030 (1996).
 - [11] P.J. Flory, “Statistical mechanics of chain molecules” (Hanser Gardner, 1989).
 - [12] See, e.g., M. Doi and S.F. Edwards, “The Theory of Polymer Dynamics” (Oxford, 1986).
 - [13] A.D. Rutenberg and M. Grant, Phys. Rev. E **64**, 21904 (2001).
 - [14] R.A. Heinzen *et al.*, Infect. Imm. **67**, 4201 (1999).
 - [15] A.S. Sechi *et al.*, J. Cell. Biol. **137**, 155 (1997).
 - [16] D. Bruns *et al.*, Neuron **28**, 205 (2000); N. Harata *et al.*, Proc. Nat. Acad. Sci., **98**, 12748 (2001); D. Schubert *et al.*, Brain. Res. **190**, 67 (1980).